


Gyrating solitons in a necklace of optical waveguides

I. V. Barashenkov 

*Centre for Theoretical and Mathematical Physics, University of Cape Town, Rondebosch 7701, South Africa
and Joint Institute for Nuclear Research, Dubna, Russia*

Daniel Feinstein

Keble College, University of Oxford, Parks Road, Oxford OX1 3PG, United Kingdom



(Received 2 November 2020; accepted 28 January 2021; published 25 February 2021)

We consider light pulses in a circular array of $2N$ coupled nonlinear optical waveguides. The waveguides are either Hermitian or alternate gain and loss in a \mathcal{PT} -symmetric fashion. Simple patterns in the array include a ring of $2N$ pulses traveling abreast and a breather—a string of pulses where all even and all odd waveguides flash in turn. In addition, the structure displays solitons gyrating around the necklace by switching from one waveguide to the next. Some of the gyrating solitons are stable while other ones are weakly unstable and evolve into gyrating multiflash strings. By tuning the gain-loss coefficient, the gyration of solitons in a non-Hermitian array may be reversed without changing the direction of their translational motion.

DOI: [10.1103/PhysRevA.103.023532](https://doi.org/10.1103/PhysRevA.103.023532)

I. INTRODUCTION

The uses of nonlinear fiber arrays for the all-optical signal processing have been recognised since the late 1980s. The multiple-channel waveguide couplers and multicore fibers can be utilized for light switching [1,2], power dividing [3], beam shaping [4], discrete diffraction management [5], spatial-division multiplexing [6], coherent beam combination, and optical pulse compression [7]. In recent years interest has been shifting to low-dimensional arrays, typically arranged in a ring [8,9]. Current applications of circular arrays include vortex-switching schemes [10,11] and generation of light beams carrying orbital angular momentum [12].

Studies of coupled waveguides have received a new impetus with the advent of the parity-time symmetry. Originally proposed in the context of the non-Hermitian quantum mechanics [13], the \mathcal{PT} symmetry proved to furnish a set of rules for the inclusion of gain and loss in fiber arrays [14] and photonic lattices [15]. The non-Hermitian optics provides light-control opportunities unattainable with traditional setups, including low-threshold switching [14,16] and unidirectional invisibility [14,17].

A circular array of waveguides is an ideal platform for the \mathcal{PT} -symmetric modification. An example of such a development is a ring-shaped necklace of $2N$ waveguides with alternating gain and loss. Reference [18] has demonstrated that the zero-amplitude state in the \mathcal{PT} -symmetric necklace remains stable as long as N is odd and the gain-loss coefficient does not exceed a finite threshold. The author of Ref. [19] has pointed out then that the stability in the necklace can be controlled by twisting it about the central axis. Further studies have concerned stationary modes in a cyclic array of \mathcal{PT} -symmetric dimers [20], a Hermitian waveguide ring with a \mathcal{PT} -symmetric impurity [21], and a multicore fiber with

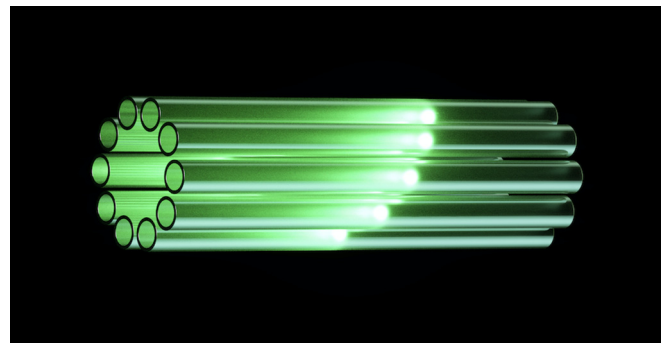


FIG. 1. A gyrating soliton in the necklace of $2N = 10$ waveguides (schematic representation).

gain in the central core and loss in the surrounding ring of waveguides [22].

With a few notable exceptions [9], studies of Hermitian and \mathcal{PT} -symmetric necklaces have been focusing on the stationary states of light. In the present work, we turn to short optical pulses. We show that the necklace of nonlinear dispersive waveguides—with or without gain and loss—supports solitons of a previously unknown kind. As these light pulses propagate along the axis of the multicore fiber, they gyrate around the necklace switching from one waveguide to another (Fig. 1).

There are several types of gyrating solitons coexisting in the array of the same number of guides. Some of these objects consist of a single pulse that spirals around the necklace; other ones comprise series of pulses of varied brightness. There are solitons with different propagation constants within each of the two varieties. While the systematic classification of stability properties of the gyrating solitons is beyond the scope

of the present study, our analysis indicates that some of these are stable.

The paper is organized as follows. In the next section (Sec. II) we classify linear supermodes in the nondispersive necklace. These serve as starting points for the bifurcating nonlinear patterns (Sec. III). In Sec. IV we consider constellations of pulses appearing simultaneously in all $2N$ waveguides, and in Secs. V and VI, we discuss solitons oscillating between even and odd subsets of the array. Solitons whose motion along the fiber is accompanied by their gyration around the necklace are introduced in Sec. VII. In the subsequent section (Sec. VIII), we consider more complex, multiflash, gyrating patterns. Stability and interaction of gyrating solitons are touched upon in Sec. IX. Section X summarizes the results of this study.

II. LINEAR NONDISPERSIVE WAVEGUIDES

The necklace of waveguides is described by the following system of $2N$ equations written in the reference frame traveling at the common group velocity [9,23]:

$$i\partial_z\psi_n + \partial_\tau^2\psi_n + \psi_{n-1} + \psi_{n+1} + 2|\psi_n|^2\psi_n = 2i\Gamma_n\psi_n. \quad (2.1)$$

Here ψ_n is the amplitude of the complex mode in the n th core ($n = 1, \dots, 2N$), z measures the length along the device, and τ is a retarded time. We are considering waveguides with an anomalous group velocity dispersion and all coefficients have been normalized to unity.

In the system (2.1) we have assumed that waveguides with gain and loss alternate:

$$\Gamma_n = (-1)^{n+1}\gamma.$$

Here $\gamma > 0$ is a common gain-loss coefficient. Skipping ahead a bit, many of our results will remain valid for the Hermitian array, $\gamma = 0$.

The equation (2.1) with $n = 1$ contains an unknown ψ_0 and the equation with $n = 2N$ includes ψ_{2N+1} . These two variables are defined by virtue of the periodicity condition:

$$\psi_{n+2N} = \psi_n.$$

We start by examining the linear nondispersive limit of (2.1) which results from dropping the nonlinearity and time derivative $\partial_\tau^2\psi_n$. Assuming a separable solution of the form $\psi_n = v_n e^{i\beta z}$, the coefficients v_n make up an eigenvector $\vec{v} = (v_1, v_2, \dots, v_{2N})^T$ of the matrix \mathcal{L} :

$$\mathcal{L}\vec{v} = \beta\vec{v},$$

where

$$\mathcal{L}_{nm} = \delta_{n,m-1} + \delta_{n,m+1} - 2i\Gamma_n\delta_{n,m}. \quad (2.2)$$

The δ symbol in (2.2) is $2N$ periodic:

$$\delta_{n,m} = \begin{cases} 1, & n = m \bmod(2N), \\ 0, & \text{otherwise.} \end{cases}$$

The eigenvalues of \mathcal{L} were determined in Ref. [18] as

$$\begin{aligned} \beta &= \pm\beta_\alpha, & \beta_\alpha &= 2\sqrt{\cos^2\left(\frac{k_\alpha}{2}\right) - \gamma^2} > 0, \\ k_\alpha &= \frac{2\pi}{N}\alpha, & \alpha &= 1, 2, \dots, N. \end{aligned} \quad (2.3)$$

The eigenvalues are all real if $\gamma \leq \gamma_c$, where

$$\gamma_c(N) = \begin{cases} 0, & N = \text{even}, \\ \sin\left(\frac{\pi}{2N}\right), & N = \text{odd}. \end{cases} \quad (2.4)$$

Note that, in the necklace with even N , the eigenvalues become complex as soon as γ is nonzero. For this reason we only consider odd N in what follows. We also assume that the symmetry is not broken, that is, $\gamma \leq \gamma_c$.

Two eigenvalues, β_N and $-\beta_N$, are simple (nonrepeated). The other $\frac{N-1}{2}$ positive and $\frac{N-1}{2}$ negative eigenvalues have algebraic multiplicity 2. Indeed, β_α coincides with $\beta_{(N-\alpha)}$ for all $\alpha = 1, 2, \dots, N-1$.

Turning to the eigenvectors of \mathcal{L} , one can readily check that

$$\vec{v}^{(\alpha)} = (e^{ik+i\theta}, e^{ik}, e^{2ik+i\theta}, e^{2ik}, \dots, e^{Nik+i\theta}, e^{Nik})^T \quad (2.5)$$

is an eigenvector corresponding to a positive eigenvalue $\beta = \beta_\alpha$. Here $k = k_\alpha$ is as in (2.3) and $\theta = \theta_\alpha$ is defined by

$$e^{i\theta_\alpha} = \frac{1 + e^{-ik_\alpha}}{2i\gamma + \beta_\alpha}, \quad \alpha = 1, 2, \dots, N.$$

It is not difficult to verify that the vectors $\vec{v}^{(\alpha)}$ and $\vec{v}^{(N-\alpha)}$ are linearly independent for all $\alpha = 1, 2, \dots, \frac{N-1}{2}$ and so each positive eigenvalue $\beta = \beta_\alpha$ has a geometric multiplicity 2.

The vector

$$\vec{w}^{(\alpha)} = (e^{ik+i\phi}, e^{ik}, e^{2ik+i\phi}, e^{2ik}, \dots, e^{Nik+i\phi}, e^{Nik})^T, \quad (2.6)$$

where $k = k_\alpha$ is as in (2.3) and $\phi = \phi_\alpha$ is defined by

$$e^{i\phi_\alpha} = \frac{1 + e^{-ik_\alpha}}{2i\gamma - \beta_\alpha}, \quad \alpha = 1, 2, \dots, N,$$

is an eigenvector associated with a *negative* eigenvalue $\beta = -\beta_\alpha$. Since the eigenvectors $\vec{w}^{(\alpha)}$ and $\vec{w}^{(N-\alpha)}$ pertaining to the equal eigenvalues $-\beta_{N-\alpha}$ and $-\beta_\alpha$ are linearly independent for any $1 \leq \alpha \leq \frac{N-1}{2}$, we conclude that each repeated negative eigenvalue of the matrix \mathcal{L} has a geometric multiplicity 2 as well.

III. NONLINEAR SELECTION RULE

Returning to the nonlinear dispersive system (2.1), we introduce a hierarchy of stretched coordinates $Z_\ell = \epsilon^\ell z$ and time scales $T_\ell = \epsilon^\ell \tau$; $\ell = 0, 1, 2, \dots$. In the limit $\epsilon \rightarrow 0$ all these variables become independent and the chain rule gives

$$\begin{aligned} \frac{\partial}{\partial z} &= D_0 + \epsilon^2 D_2 + \epsilon^4 D_4 + \dots, \\ \frac{\partial}{\partial \tau} &= \partial_0 + \epsilon \partial_1 + \epsilon^2 \partial_2 + \dots, \end{aligned}$$

where $D_\ell = \partial/\partial Z_\ell$ and $\partial_\ell = \partial/\partial T_\ell$. Symmetry considerations suggest that the complex modes ψ_n should not depend on the odd coordinates Z_1, Z_3, \dots ; this is why we have omitted the odd terms in the expansion of ∂_z . Expanding

$$\psi_n = \epsilon A_n + \epsilon^3 B_n + \dots$$

and substituting into (2.1), we equate coefficients of like powers of ϵ .

The order ϵ^1 gives

$$iD_0\vec{A} + \mathcal{L}\vec{A} = 0, \quad (3.1)$$

where $\vec{A} = (A_1, A_2, \dots, A_{2N})^T$ and we have assumed that \vec{A} does not change on the fast time scale, T_0 . The general solution of (3.1) is given by a linear combination:

$$\vec{A} = \sum_{\alpha=1}^N p^{(\alpha)} \vec{v}^{(\alpha)} e^{i\beta_\alpha z} + \sum_{\alpha=1}^N r^{(\alpha)} \vec{w}^{(\alpha)} e^{-i\beta_\alpha z}, \quad (3.2)$$

where the constant vectors $\vec{v}^{(\alpha)}$ and $\vec{w}^{(\alpha)}$ are as in (2.5) and (2.6) while the scalar coefficients $p^{(\alpha)}$ and $r^{(\alpha)}$ are assumed to depend on the “slow” variables Z_2, Z_4, \dots and T_1, T_2, \dots . The individual terms in (3.2) are commonly referred to as supermodes. The sum (3.2) with a specific choice of coefficients is called a “linear pattern” in what follows.

To determine nonlinear constraints that select particular linear patterns in the necklace, we proceed to the order ϵ^3 which gives a nonhomogeneous system of equations for coefficients B_n :

$$iD_0 \vec{B} + \mathcal{L} \vec{B} = \vec{\mathcal{R}}, \quad (3.3)$$

where

$$\mathcal{R}_n = -(iD_2 + \partial_1^2 + 2|A_n|^2)A_n,$$

$n = 1, 2, \dots, 2N$. The vector function $\vec{\mathcal{R}}$ will generally have terms that are in resonance with the “frequencies” of the linear nondispersive system. The unbounded growth of the coefficients B_n as $z \rightarrow \infty$ (and the resulting breakdown of the asymptotic expansion) can only be avoided if $\vec{\mathcal{R}}$ is orthogonal to the eigenvectors of the matrix \mathcal{L} . These orthogonality relations (a) select the linear patterns that persist in the nonlinear dispersive regime when the amplitudes of the complex modes are no longer small and the beams are no longer stationary and (b) determine the longitudinal structure and temporal evolution of nonlinear pulses of light.

In the subsequent sections we go over several possible choices in (3.2).

IV. SIMULTANEOUS PULSES IN 2N GUIDES

Circular-symmetric distributions of the power $|\psi_n|^2$ result by keeping only one supermode in the linear pattern (3.2). Choosing

$$\vec{A} = p \vec{v}^{(N)} e^{i\beta z}, \quad (4.1)$$

where $\beta = \beta_N$ and $p = p^{(N)}$, a bounded solution to Eq. (3.3) (if one exists) will have the form

$$\vec{B} = \vec{\mathcal{X}} e^{i\beta z}, \quad (4.2)$$

where $\vec{\mathcal{X}}$ satisfies

$$(\mathcal{L} - \beta I) \vec{\mathcal{X}} = -(iD_2 p + \partial_1^2 p + 2|p|^2 p) \vec{v}^{(N)}. \quad (4.3)$$

The singular system (4.3) admits a solution if and only if its right-hand side is orthogonal to the eigenvector $\vec{v}^{(N)}$ in the sense of the dot product

$$\vec{y} \cdot \vec{z} = \sum_{n=1}^{2N} y_n z_n. \quad (4.4)$$

[In Eq. (4.4), \vec{y} and \vec{z} are vectors with complex components.] Making use of the identity

$$\vec{v}^{(\alpha)} \cdot \vec{v}^{(\alpha)} = (1 + e^{i\theta_N}) N \delta_{\alpha, N}, \quad (4.5)$$

with $\alpha = N$, the solvability condition reduces to the nonlinear Schrödinger equation

$$i \frac{\partial p}{\partial Z_2} + \frac{\partial^2 p}{\partial T_1^2} + 2|p|^2 p = 0. \quad (4.6)$$

A localized solution of Eq. (4.6) is the soliton

$$p = e^{iZ_2} \operatorname{sech} T_1, \quad (4.7)$$

where the amplitude has been set equal to 1. (There is no loss in generality in setting the amplitude to unity as it only appears as a coefficient in front of ϵ when the solution is expressed in the original coordinates.) The vector function (4.1) with p as in (4.7) describes identical light pulses traveling level with each other in $2N$ waveguides. All waveguides shine in unison and with the same intensity: $|\psi_n|^2 = \epsilon^2 \operatorname{sech}^2(\epsilon \tau)$.

Another simultaneous ring of pulses results by letting $r^{(\alpha)} = 0$ for all $\alpha = 1, \dots, N$, and $p^{(\alpha)} = 0$ for all α except one particular value $\alpha = \alpha_0$ and its symmetric partner $\alpha = N - \alpha_0$. Here $1 \leq \alpha_0 \leq \frac{N-1}{2}$. Denoting

$$p^{(\alpha_0)} \equiv p, \quad p^{(N-\alpha_0)} \equiv q, \quad \vec{v}^{(\alpha_0)} \equiv \vec{v}, \quad \vec{v}^{(N-\alpha_0)} \equiv \vec{u},$$

and $\beta_{\alpha_0} = \beta$, the linearized pattern (3.2) becomes

$$\vec{A} = (p \vec{v} + q \vec{u}) e^{i\beta z}. \quad (4.8)$$

A bounded third-order correction B_n has the form (4.2), where the vector $\vec{\mathcal{X}}$ satisfies the system

$$\sum_{m=1}^{2N} \mathcal{L}_{nm} \mathcal{X}_m - \beta \mathcal{X}_n = -F v_n - G u_n - 2[q^2 p^* u_n^2 v_n^* + p^2 q^* v_n^2 u_n^*], \quad (4.9)$$

with the coefficient functions

$$F(Z_2, \dots, T_1, \dots) = (iD_2 + \partial_1^2 + 2|p|^2 + 4|q|^2)p, \quad (4.10)$$

$$G(Z_2, \dots, T_1, \dots) = (iD_2 + \partial_1^2 + 4|p|^2 + 2|q|^2)q. \quad (4.11)$$

Since the zero eigenvalue of the matrix $\mathcal{L} - \beta I$ in the left-hand side of (4.9) has geometric multiplicity 2, the nonhomogeneous system (4.9) has two solvability conditions. Taking the scalar product of its right-hand side with \vec{u} and \vec{v} produces a pair of amplitude equations:

$$i \frac{\partial p}{\partial Z_2} + \frac{\partial^2 p}{\partial T_1^2} + 2(|p|^2 + 2|q|^2)p = 0, \quad (4.12a)$$

$$i \frac{\partial q}{\partial Z_2} + \frac{\partial^2 q}{\partial T_1^2} + 2(|q|^2 + 2|p|^2)q = 0. \quad (4.12b)$$

In obtaining the system (4.12), we used the following two identities in addition to the identity (4.5):

$$\vec{v}^{(\alpha)} \cdot \vec{v}^{(N-\alpha)} = (e^{i(k_\alpha + 2\theta_\alpha)} + 1)N,$$

$$\sum_{n=1}^{2N} v_n^3 u_n^* = \sum_{n=1}^{2N} u_n^3 v_n^* = 0. \quad (4.13)$$

The power distribution associated with a repeated eigenvalue β_{α_0} is z -independent but not uniform across the necklace. Letting, for simplicity, $p = q$, Eq. (4.8) gives

$$|A_n|^2 = 2|p|^2 [1 + \cos(nk_{\alpha_0})].$$

A localized pattern arises when the soliton solution of (4.12) is chosen:

$$p = q = \frac{1}{\sqrt{3}} e^{iZ_2} \operatorname{sech} T_1. \quad (4.14)$$

The vector (4.8) with p and q as in (4.14) describes a ring-shaped constellation of light pulses traveling abreast in $2N$ fibers. The pulse power undergoes a sinusoidal variation along the ring.

Earlier studies of simultaneous pulses in circular arrays of coupled Hermitian waveguides were reported in Refs. [18,24,25]. In Ref. [25], rings of solitonic pulses with varying power were described as bifurcations of the uniformly powered ring. Our perspective here is different; we have considered simultaneous pulses as nonlinear perturbations of nonuniform linear patterns.

V. UNIFORM BREATHERS

Keeping terms with both positive and negative propagation constants in the linear pattern (3.2) gives rise to z -dependent power distributions. The simplest possibility corresponds to retaining just two terms:

$$\vec{A} = p\vec{v}e^{i\beta z} + q\vec{w}e^{-i\beta z}. \quad (5.1)$$

Here $\beta = \beta_N$ is a simple positive eigenvalue, while

$$\vec{v} = \vec{v}^{(N)}, \quad \vec{w} = \vec{w}^{(N)}$$

are the eigenvectors corresponding to β_N and its negative, respectively. With this choice, the bounded solution of Eq. (3.3) is

$$\vec{B} = \vec{X}e^{i\beta z} + \vec{Y}e^{-i\beta z} + \vec{M}e^{3i\beta z} + \vec{N}e^{-3i\beta z}, \quad (5.2)$$

where the amplitudes \vec{X} and \vec{Y} satisfy nonhomogeneous algebraic equations with singular matrices:

$$(\mathcal{L} - \beta I)\vec{X} = -F\vec{v}, \quad (5.3)$$

$$(\mathcal{L} + \beta I)\vec{Y} = -G\vec{w}. \quad (5.4)$$

Here F and G are as in (4.10) and (4.11).

Equation (5.3) admits a solution if and only if its right-hand side is orthogonal to \vec{v} while the right-hand side of (5.4) should be orthogonal to \vec{w} . [Here orthogonality is understood in the sense of the dot product (4.4).] Using (4.5) and the identity

$$\vec{w}^{(\alpha)} \cdot \vec{w}^{(\alpha)} = (1 + e^{i\phi_N})N\delta_{\alpha,N},$$

with $\alpha = N$, these orthogonality constraints translate into Eqs. (4.12).

Letting $q = p$, Eq. (5.1) gives rise to an oscillatory power distribution:

$$|A_{2m-1}|^2 = 4|p|^2 \sin^2(\beta z + \theta_N),$$

$$|A_{2m}|^2 = 4|p|^2 \cos^2(\beta z),$$

$m = 1, 2, \dots, N$. This describes a flashing necklace: all odd waveguides blink in unison and all even waveguides reach their maximum power at the same z , but there is a lag between the odd and the even guides. Note that the flashing is uniform: the maximum power is the same for all waveguides.

The soliton solution (4.14) of the system (4.12) provides an envelope for a finite-duration sequence of short flashes in

the necklace—a spatiotemporal pattern commonly referred to as a breather. Breathers in fiber directional couplers (that is, in necklaces consisting just of two waveguides, with no gain or loss) have been described numerically and variationally [26]. For the asymptotic descriptions and non-Hermitian extensions, see Ref. [27].

VI. NONUNIFORM FLASHING

A set of slightly more complex patterns results by letting, in Eq. (3.2), $r^{(\alpha)} = 0$ and $p^{(\alpha)} = 0$ for all $\alpha = 1, 2, \dots, N$ except one particular value, $\alpha = \alpha_0$ ($1 \leq \alpha_0 \leq \frac{N-1}{2}$), and its symmetric partner, $\alpha = N - \alpha_0$. Denoting

$$p^{(\alpha_0)} \equiv p_1, \quad r^{(\alpha_0)} \equiv q_1, \quad r^{(N-\alpha_0)} \equiv p_2, \quad p^{(N-\alpha_0)} \equiv q_2,$$

and $\beta_{\alpha_0} = \beta$, Eq. (3.2) becomes

$$\vec{A} = \vec{\eta}e^{i\beta z} + \vec{\xi}e^{-i\beta z}, \quad (6.1a)$$

where

$$\vec{\eta} = p_1\vec{v}^{(\alpha_0)} + q_2\vec{v}^{(N-\alpha_0)}, \quad \vec{\xi} = q_1\vec{w}^{(\alpha_0)} + p_2\vec{w}^{(N-\alpha_0)}. \quad (6.1b)$$

The next-order correction has the form (5.2), where \vec{X} and \vec{Y} satisfy

$$(\mathcal{L} - \beta I)\vec{X} = -\vec{F}, \quad (6.2)$$

$$(\mathcal{L} + \beta I)\vec{Y} = -\vec{G}, \quad (6.3)$$

with

$$\mathcal{F}_n = iD_2\eta_n + \partial_1^2\eta_n + 2(|\eta_n|^2 + 2|\xi_n|^2)\eta_n,$$

$$\mathcal{G}_n = iD_2\xi_n + \partial_1^2\xi_n + 2(2|\eta_n|^2 + |\xi_n|^2)\xi_n.$$

The zero eigenvalue of the matrix $\mathcal{L} - \beta I$ in Eq. (6.2) has geometric multiplicity 2, and the same is true for the zero eigenvalue of the matrix $\mathcal{L} + \beta I$ in (6.3). Evaluating the dot product of the right-hand side of (6.2) with the vectors $\vec{v}^{(\alpha_0)}$ and $\vec{v}^{(N-\alpha_0)}$, and then taking the product of the right-hand side of (6.3) with $\vec{w}^{(\alpha_0)}$ and $\vec{w}^{(N-\alpha_0)}$, we arrive at a system of four amplitude equations:

$$\begin{aligned} i\frac{\partial p_\mu}{\partial Z_2} + \frac{\partial^2 p_\mu}{\partial T_1^2} + 2(|p_\mu|^2 + 2|p_{\mu+1}|^2)p_\mu \\ + 4(|q_1|^2 + |q_2|^2)p_\mu + 4q_1q_2p_{\mu+1}^* \\ = 0, \end{aligned} \quad (6.4a)$$

$$\begin{aligned} i\frac{\partial q_\mu}{\partial Z_2} + \frac{\partial^2 q_\mu}{\partial T_1^2} + 2(|q_\mu|^2 + 2|q_{\mu+1}|^2)q_\mu \\ + 4(|p_1|^2 + |p_2|^2)q_\mu + 4p_1p_2q_{\mu+1}^* \\ = 0, \end{aligned} \quad (6.4b)$$

where $\mu = 1$ and 2 . In (6.4), we use the cyclic notation for the indices: p_3 should be understood as p_1 and q_3 as q_1 .

The system (6.4) is invariant under a three-parameter transformation:

$$q_\mu \rightarrow e^{i\varphi_\mu}q_\mu, \quad p_\mu \rightarrow e^{i\vartheta_\mu}p_\mu \quad (\mu = 1, 2), \quad (6.5a)$$

where $\varphi_{1,2}$ and $\vartheta_{1,2}$ are four constant angles satisfying

$$\varphi_1 + \varphi_2 = \vartheta_1 + \vartheta_2. \quad (6.5b)$$

Solutions that are related by the transformation (6.5) will be regarded as equivalent.

It is convenient to introduce vector notation for the four-component columns:

$$\Phi = \begin{pmatrix} p_1 \\ p_2 \\ q_1 \\ q_2 \end{pmatrix}.$$

There are $\binom{4}{2} = 6$ nonequivalent soliton solutions with two nonzero components:

$$\begin{aligned} \Phi^{(12)} &= \begin{pmatrix} 1 \\ 0 \\ 0 \\ 1 \end{pmatrix} f, & \Phi^{(21)} &= \begin{pmatrix} 0 \\ 1 \\ 1 \\ 0 \end{pmatrix} f, & \Phi^{(11)} &= \begin{pmatrix} 1 \\ 0 \\ 1 \\ 0 \end{pmatrix} f, \\ \Phi^{(22)} &= \begin{pmatrix} 0 \\ 1 \\ 0 \\ 1 \end{pmatrix} f, & \Phi^{(p)} &= \begin{pmatrix} 1 \\ 1 \\ 0 \\ 0 \end{pmatrix} f, & \Phi^{(q)} &= \begin{pmatrix} 0 \\ 0 \\ 1 \\ 1 \end{pmatrix} f. \end{aligned}$$

Here, f accounts for the large-scale space-time variation of the pattern:

$$f(Z_2, T_1) = \frac{1}{\sqrt{3}} e^{iZ_2} \operatorname{sech} T_1. \quad (6.6)$$

The solution $\Phi^{(12)}$ reproduces Eq. (4.8) with p and q as in (4.14). This solution as well as $\Phi^{(21)}$ describe constellations of $2N$ pulses traveling abreast, with their power varying along the necklace. On the other hand, $\Phi^{(11)}$ and $\Phi^{(22)}$ define uniformly flashing patterns similar to (5.1).

Deferring the interpretation of $\Phi^{(p)}$ and $\Phi^{(q)}$ to the next section, here we consider two more soliton solutions of the system (6.4). All the components of both solutions are nonzero:

$$\Phi^{(A)} = \frac{1}{\sqrt{3}} \begin{pmatrix} 1 \\ 1 \\ 1 \\ 1 \end{pmatrix} f, \quad \Phi^{(B)} = \sqrt{\frac{3}{5}} \begin{pmatrix} 1 \\ 1 \\ 1 \\ -1 \end{pmatrix} f, \quad (6.7)$$

where $f(Z_2, T_1)$ is as in (6.6).

The power load of individual waveguides associated with the solution $\Phi^{(A)}$ is given by

$$\begin{aligned} |A_{2m-1}|^2 &= \frac{16}{3} |f|^2 \cos^2 \left(\frac{2m-1}{2} k \right) \\ &\quad \times \sin^2 \left(\beta z + \theta + \frac{k}{2} \right), \\ |A_{2m}|^2 &= \frac{16}{3} |f|^2 \cos^2(mk) \cos^2(\beta z), \end{aligned} \quad (6.8)$$

while the soliton $\Phi^{(B)}$ carries the following power distribution:

$$\begin{aligned} |A_{2m-1}|^2 &= \frac{12}{5} |f|^2 + \frac{12}{5} |f|^2 \sin[(2m-1)k] \\ &\quad \times \sin(2\beta z + 2\theta + k), \\ |A_{2m}|^2 &= \frac{12}{5} |f|^2 - \frac{12}{5} |f|^2 \sin(2mk) \sin(2\beta z). \end{aligned} \quad (6.9)$$

In either of these equations, $\beta = \beta_{\alpha_0}$, $k = k_{\alpha_0}$, and $\theta = \theta_{\alpha_0}$, while m changes from 1 to N . Both (6.8) and (6.9) repre-

sent flashing patterns, or breathers, where all odd and all even waveguides flash synchronously. The maximum power attainable in an individual waveguide undergoes a sinusoidal variation along the necklace.

VII. GYRATING SOLITONS

A. Single-frequency pattern

The solitons $\Phi^{(p)}$ and $\Phi^{(q)}$ represent light pulses gyrating around the necklace.

The power distribution associated with $\Phi^{(p)}$ has the form of a spiral wave [Fig. 2(a)]:

$$\begin{aligned} |A_{2m-1}|^2 &= 4|f|^2 \sin^2(km + \beta z + \theta), \\ |A_{2m}|^2 &= 4|f|^2 \cos^2(km + \beta z). \end{aligned} \quad (7.1)$$

Here $m = 1, 2, \dots, N$ and the parameters are $k = k_\alpha$, $\beta = \beta_\alpha$, and $\theta = \theta_\alpha$. To simplify the notation, we have dropped the subscript 0 from the index α ($1 \leq \alpha \leq \frac{N-1}{2}$).

To establish whether the soliton is gyrating clockwise or counterclockwise, we need to determine which of the two neighbors of the $2m$ th waveguide will flash immediately after the $2m$ th guide has. Assume that the $2m$ th waveguide attains its maximum power at the point $z = z_0$. Then the closest maximum of $|A_{2m+1}|^2$ to the right of z_0 is at $z = z_0 + \Delta_{2m+1}$, and the nearest maximum of $|A_{2m-1}|^2$ to the right of z_0 is at $z = z_0 + \Delta_{2m-1}$, where the delay intervals are given by

$$\Delta_{2m+1} = \frac{1}{\beta} \left(\frac{\pi}{2} - \theta - k \right) \quad (7.2)$$

and

$$\Delta_{2m-1} = \begin{cases} -\frac{1}{\beta} \left(\frac{\pi}{2} + \theta \right) & \text{if } \theta < -\frac{\pi}{2}, \\ \frac{1}{\beta} \left(\frac{\pi}{2} - \theta \right) & \text{if } \theta > -\frac{\pi}{2}. \end{cases} \quad (7.3)$$

Comparing the lags (7.2) and (7.3) one can readily check that the $(2m+1)$ th guide flashes sooner, respectively later, than the $(2m-1)$ th one if $\gamma < \gamma_\alpha$, respectively $\gamma > \gamma_\alpha$, where

$$\gamma_\alpha = \cos^2 \frac{k_\alpha}{2}.$$

Let

$$\alpha_c(N) = \text{floor} \left[\frac{N}{\pi} \arccos(\gamma_c^{1/2}) \right], \quad (7.4)$$

where $\text{floor}[x]$ stands for the greatest integer less than or equal to x , while $\gamma_c = \sin^2(\frac{\pi}{2N})$ is the linear \mathcal{PT} -symmetry-breaking threshold given by Eq. (2.4). For all $\alpha \leq \alpha_c$ we have $\gamma_\alpha \geq \gamma_c$. Since we are considering a necklace operating in the stable regime ($\gamma \leq \gamma_c$), then, assuming that the waveguides are numbered against the clock, we conclude that the soliton $\Phi^{(p)}$ with any $\alpha = 1, 2, \dots, \alpha_c$, and regardless of γ , is gyrating counterclockwise.

By contrast, the sense of gyration of the soliton $\Phi^{(p)}$ with $\alpha = \alpha_c + 1, \dots, \frac{N-1}{2}$ does depend on γ . The corresponding transition values γ_α lie under the \mathcal{PT} -symmetry-breaking threshold. When $0 \leq \gamma < \gamma_\alpha$, the soliton gyrates counterclockwise, but when $\gamma_\alpha < \gamma < \gamma_c$, it revolves in the clockwise direction. This crossover is illustrated by Fig. 3.

The behavior of the solitons $\Phi^{(q)}$ is opposite to that of $\Phi^{(p)}$. Namely, pulses with $\alpha = 1, 2, \dots, \alpha_c$ are gyrating clockwise

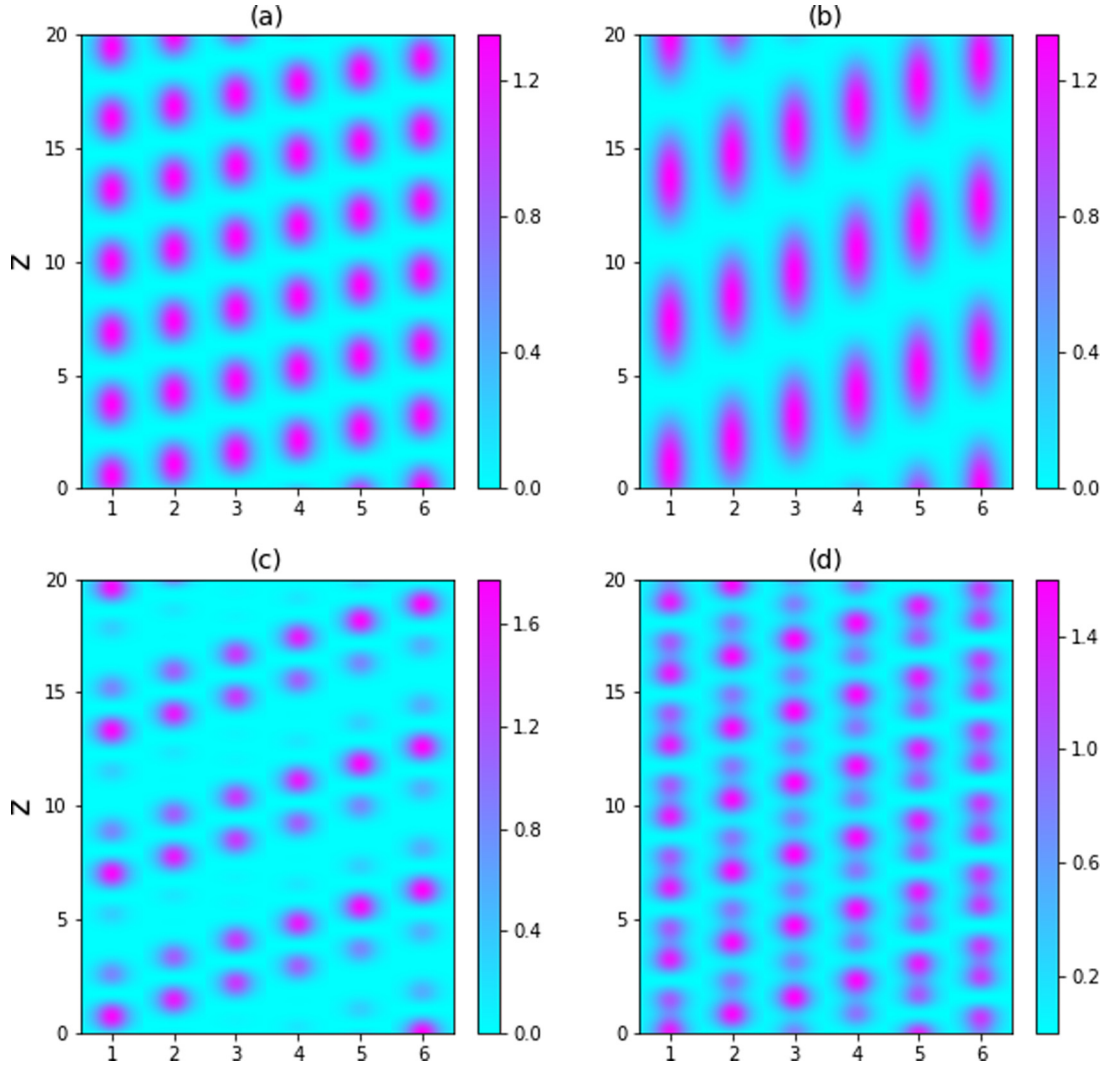


FIG. 2. Four types of gyrating solitons in a necklace of $2N = 6$ waveguides. Each panel consists of six vertical lanes displaying the (τ, z) distribution of optical power in six waveguides. The horizontal side of each lane represents a short period of time, $-20 < \tau < 20$; the τ axis is not marked or labeled. The vertical coordinate measures the length along the waveguides, with $0 \leq z \leq 20$. (a) Jiver soliton (7.5). The panel shows the power distribution (7.1). (b) The power density (7.7) corresponding to the waltzer (7.8). (c) Power distribution (8.1) associated with the multiflash gyration A . (d) Power pattern (8.2) of the multiflash solution B . In all panels, $\gamma = 0$ and $\alpha = 1$. All solitons have the inverse-width parameter $\epsilon = 0.1$.

for all γ . Those with $\alpha = \alpha_c + 1, \dots, \frac{N-1}{2}$ are also revolving clockwise for small γ , but their direction of gyration can be reversed by raising γ above γ_α .

The two gyrating solitons whose linear patterns are given by Eq. (6.1), with the coefficients defined by the vector $\Phi^{(p)}$ or $\Phi^{(q)}$, can be written in a unified way as

$$\vec{\psi} = \epsilon \frac{\vec{v}^{(\alpha)} e^{i\beta_\alpha z} + \vec{w}^{(N-\alpha)} e^{-i\beta_\alpha z}}{\sqrt{3}} e^{i\epsilon^2 z} \text{sech}(\epsilon \tau) + O(\epsilon^3), \quad (7.5)$$

where $1 \leq \alpha \leq N - 1$. Solitons with $\alpha = N - \alpha_c, \dots, N - 1$ are gyrating clockwise and those with $\alpha = 1, \dots, \alpha_c$ are moving against the clock. For $\alpha = \alpha_c + 1, \dots, N - \alpha_c - 1$, the direction of gyration is controlled by the choice of γ .

Before turning to other types of gyrating pulses we note two more characteristics of the solitons (7.5) that can be controlled in the non-Hermitian situation. Namely, by varying

the gain-loss coefficient one can change the length of the pulse and its period of revolution around the necklace. Both of these quantities are given by the z period of the power density (7.1). The length of two particular pulses with $\alpha = \frac{N \pm 1}{2}$ can even be sent to infinity—one just needs to tune γ to γ_c . (The reason is that the propagation constant $\beta_{(N \pm 1)/2} \rightarrow 0$ as $\gamma \rightarrow \gamma_c$.)

Figure 3 exemplifies the change in the flash duration with a sequence of four values of γ from the interval $(0, \gamma_c)$.

B. Two-frequency pattern

A quasiperiodic pattern that does not fit into the general ansatz (6.1) combines eigenvectors associated with a repeated and a single eigenvalue:

$$\vec{A} = p \vec{v}^{(\alpha)} e^{i\beta_\alpha z} + q \vec{v}^{(N)} e^{i\beta_N z}. \quad (7.6)$$

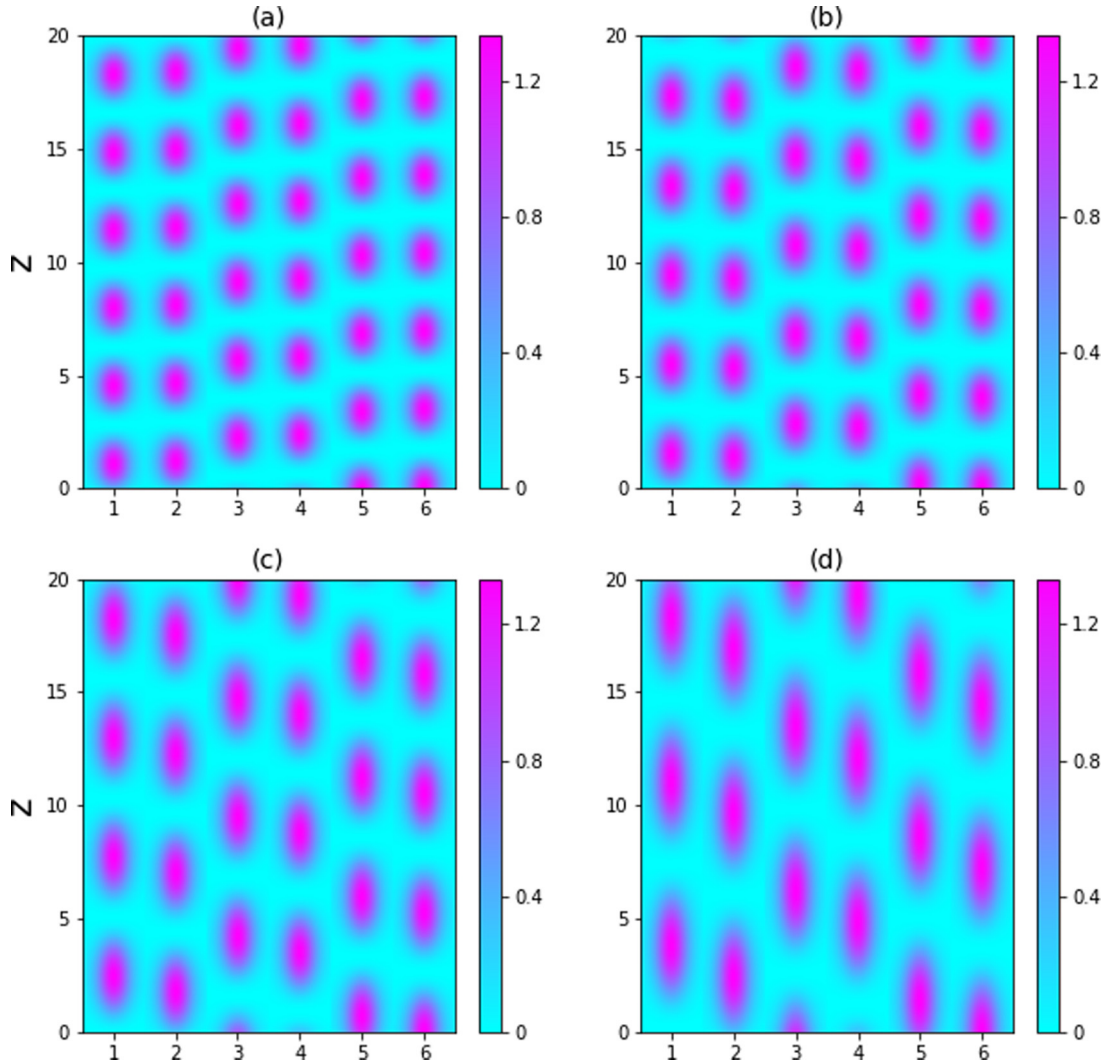


FIG. 3. The transition from counterclockwise to clockwise gyration in the necklace of six waveguides. All four panels pertain to the same jiver soliton as in Fig. 2(a) but with different γ . As in Fig. 2, each panel consists of six vertical lanes. The n th lane shows $|A_n(\tau, z)|^2$, the power density in the n th waveguide. The horizontal side of each lane represents a short period of time, $-20 < \tau < 20$, with the τ axis not marked or labeled. The vertical coordinate measures the length along the waveguides. All four power distributions are given by Eq. (7.1), where $\alpha = 1$ and $\epsilon = 0.1$, while γ varies: (a) $\gamma = 0.20$, (b) $\gamma = 0.30$, (c) $\gamma = 0.40$, and (d) $\gamma = 0.45$. The transition occurs as γ is raised through $\gamma_1 = 0.25$.

Here α is an arbitrarily chosen mode number, $1 \leq \alpha \leq N - 1$. With this choice, the right-hand side of Eq. (3.3) features two resonant terms proportional to $e^{i\beta_\alpha z}$ and $e^{i\beta_N z}$, respectively. Since β_α is a repeated eigenvalue, the former term imposes two solvability conditions. With the help of (4.5), we verify that one of these is trivially satisfied. The other solvability condition and the solvability constraint associated with the propagation constant β_N constitute the system (4.12). [The derivation makes use of the identities (4.5) and (4.13).]

Like the distribution (7.1) before, the power density associated with the pattern (7.6) has the form of a spiral:

$$|A_{2m-1}|^2 = 4|p|^2 \cos^2 \left[\frac{k_\alpha m + (\beta_\alpha - \beta_N)z + \theta_\alpha - \theta_N}{2} \right],$$

$$|A_{2m}|^2 = 4|p|^2 \cos^2 \left[\frac{k_\alpha m + (\beta_\alpha - \beta_N)z}{2} \right]. \quad (7.7)$$

Here $m = 1, 2, \dots, N$ and we have assumed a simple reduction of the system (4.12): $p = q$. [See Fig. 2(b).] A localized pattern corresponds to the soliton solution of that system, Eq. (4.14).

The self-contained form of the solution whose linear order is given by Eq. (7.6), with p and q as in (4.14), is

$$\vec{\psi} = \epsilon \frac{\vec{v}^{(\alpha)} e^{i\beta_\alpha z} + \vec{v}^{(N)} e^{i\beta_N z}}{\sqrt{3}} e^{i\epsilon^2 z} \operatorname{sech}(\epsilon \tau) + O(\epsilon^3). \quad (7.8)$$

This is another gyrating soliton, different from (7.5). An argument similar to the one in Sec. VII A shows that the solitons (7.8) with $\alpha \geq \frac{N+1}{2}$ are gyrating clockwise, while those with $\alpha \leq \frac{N-1}{2}$ are moving against the clock.

Figures 2(a) and 2(b) illustrate the difference between the two types of gyrating solitons in the Hermitian necklace of six waveguides. The period of revolution around the necklace associated with the spiral pattern (7.7) is longer than that of the pattern (7.1). By the time the soliton (7.8) completes just

one round of its “waltz” around the necklace, its more agile counterpart (7.5) will have “jived” around twice. For ease of reference, we dub the gyrating solitons (7.5) and (7.8) the *jiver* and the *waltzer*, respectively.

VIII. MULTIFLASH GYRATION

When the waveguides are linear and nondispersive, that is, when the necklace is described by the system (2.1) with neither cubic nor time-derivative terms included, any set of coefficients $p^{(\alpha)}$ and $r^{(\alpha)}$ in (3.2) defines a pattern in the necklace. However, only a handful of those patterns persist after the addition of nonlinear and dispersive terms to (3.2).

In this section we identify two more spiral patterns associated with gyrating solitons. The patterns in question generalize the two-mode combination (7.6). They involve an eigenvector $\vec{v}^{(\alpha)}$ associated with a repeated eigenvalue β_α (where $1 \leq \alpha \leq N - 1$), its mirror-reflected counterpart $\vec{w}^{(N-\alpha)}$ associated with the negative propagation constant $-\beta_\alpha$, and the eigenvectors $\vec{v}^{(N)}$ and $\vec{w}^{(N)}$ corresponding to the pair of single eigenvalues $\pm\beta_N$:

$$\vec{A} = p_1 \vec{v}^{(\alpha)} e^{i\beta_\alpha z} + p_2 \vec{w}^{(N-\alpha)} e^{-i\beta_\alpha z} + q_1 \vec{v}^{(N)} e^{i\beta_N z} + q_2 \vec{w}^{(N)} e^{-i\beta_N z}.$$

This time, the right-hand side of Eq. (3.3) has four resonant terms proportional to $e^{\pm i\beta_\alpha z}$ and $e^{\pm i\beta_N z}$. Two of the six solvability conditions are satisfied automatically while the remaining four amount to the system (6.4).

Two nonequivalent solutions of the system (6.4) with all components different from zero are given by Eqs. (6.7). The power distribution associated with the solution $\Phi^{(A)}$ has the form

$$|A_{2m-1}|^2 = \frac{4}{3} |f|^2 [\sin(\beta_N z + \theta_N) + \sin(mk_\alpha + \beta_\alpha z + \theta_\alpha)]^2, \\ |A_{2m}|^2 = \frac{4}{3} |f|^2 [\cos(\beta_N z) + \cos(mk_\alpha + \beta_\alpha z)]^2. \quad (8.1)$$

Here $m = 1, 2, \dots, N$, and the slowly changing amplitude f is given by (6.6). The power distribution (8.1) describes several flashes of unequal brightness appearing in rapid succession. The string of pulses gyrates around the necklace as a whole, with the ordering of bright and dim flashes changing from one waveguide to another.

Figure 2(c) illustrates a multiflash string (8.1) in a necklace of $2N = 6$ guides. In this case the string comprises a bright flash and one or two dim pulses appearing short distances apart. In waveguides on one side of the necklace, the bright flash comes before the dim signal and on the other side the bright pulse follows the dim one.

The power distribution corresponding to the solution $\Phi^{(B)}$ is

$$|A_{2m-1}|^2 = \frac{12}{5} |f|^2 [\cos^2(\beta_N z + \theta_N) + \sin^2(mk_\alpha + \beta_\alpha z + \theta_\alpha)], \\ |A_{2m}|^2 = \frac{12}{5} |f|^2 [\sin^2(\beta_N z) + \cos^2(mk_\alpha + \beta_\alpha z)]. \quad (8.2)$$

Here $m = 1, 2, \dots, N$, and the coefficient function f is as in (6.6). Like the power pattern (8.1), the distribution (8.2) describes a multiflash string gyrating around the necklace [see Fig. 2(d)].

Although the multiflash patterns have power distributions more complex than those of the spirals (7.1) and (7.7), they play an important role in the dynamics of the necklace. Numerical simulations indicate that the multiflash gyrating strings may emerge as products of the evolution of the unstable single-pulse gyrators (7.1). (See Sec. IX A below.)

For future reference, we reproduce the multiflash gyrating solitons in a self-contained form:

$$\vec{\psi}_A = \epsilon (\vec{v}^{(\alpha)} e^{i\beta_\alpha z} + \vec{w}^{(N-\alpha)} e^{-i\beta_\alpha z} + \vec{v}^{(N)} e^{i\beta_N z} + \vec{w}^{(N)} e^{-i\beta_N z}) \frac{e^{i\epsilon^2 z}}{3} \operatorname{sech}(\epsilon \tau) + O(\epsilon^3), \quad (8.3)$$

$$\vec{\psi}_B = \epsilon (\vec{v}^{(\alpha)} e^{i\beta_\alpha z} + \vec{w}^{(N-\alpha)} e^{-i\beta_\alpha z} + \vec{v}^{(N)} e^{i\beta_N z} - \vec{w}^{(N)} e^{-i\beta_N z}) \frac{e^{i\epsilon^2 z}}{\sqrt{5}} \operatorname{sech}(\epsilon \tau) + O(\epsilon^3). \quad (8.4)$$

As the notation suggests, we call (8.3) and (8.4) the *A*- and *B*-multiflash gyrator, respectively.

IX. SOLITON DYNAMICS

A. Stability and scattering of gyrating solitons

The comprehensive stability analysis of gyrating solitons is beyond the scope of the present study. Here, we restrict ourselves to a few sets of numerical simulations verifying that these objects do not blow up, disperse, or transmute into nongyrating localized structures within a short period of time.

All our computer simulations were carried out on the necklace of six waveguides ($N = 3$). We considered the system (2.1) in both the Hermitian ($\gamma = 0$) and the \mathcal{PT} -symmetric ($\gamma \neq 0$) situation.

Our first series of simulations involved the “jiving” soliton, Eq. (7.5) with $\alpha = 1$ [Fig. 2(a)]. The jiver was found to be weakly unstable, both for $\gamma = 0$ and $\gamma \neq 0$. Choosing the initial condition in the form (7.5) with $\epsilon = 0.1$ or $\epsilon = 0.2$, and neglecting the $O(\epsilon^3)$ terms, the resulting oscillatory solution was seen to slowly evolve into the multiflash solution (8.3). The pattern shown in Fig. 2(a) would gradually transform into the density profile of Fig. 2(c).

By contrast, the “waltzing” soliton in the same system has turned out to be stable for all values of γ that we examined, including $\gamma = 0$. Random noise added to the initial condition in the form (7.8), with $\alpha = 1$ and $\epsilon = 0.1$ or 0.2 , did not produce any measurable growth of the perturbation. The pattern shown in Fig. 2(b) would remain visibly unchanged.

It is instructive to compare the interaction of two jivers to the scattering of two waltzing solitons. We note that the system (2.1) has the Galilei invariance; namely, if $\psi_n(\tau, z)$ is a solution, then so is

$$\tilde{\psi}_n(\tau, z) \equiv e^{i\frac{V}{2}(\tau - \frac{V}{2}z)} \psi_n(\tau - Vz, z).$$

In particular, if ψ is a quiescent, unmoving, soliton, then $\tilde{\psi}$ gives the pulse traveling with the velocity V .

Making use of the Galilei transformation we set up an initial condition for the collision of two clockwise-gyrating jivers with equal amplitudes and equal oppositely directed

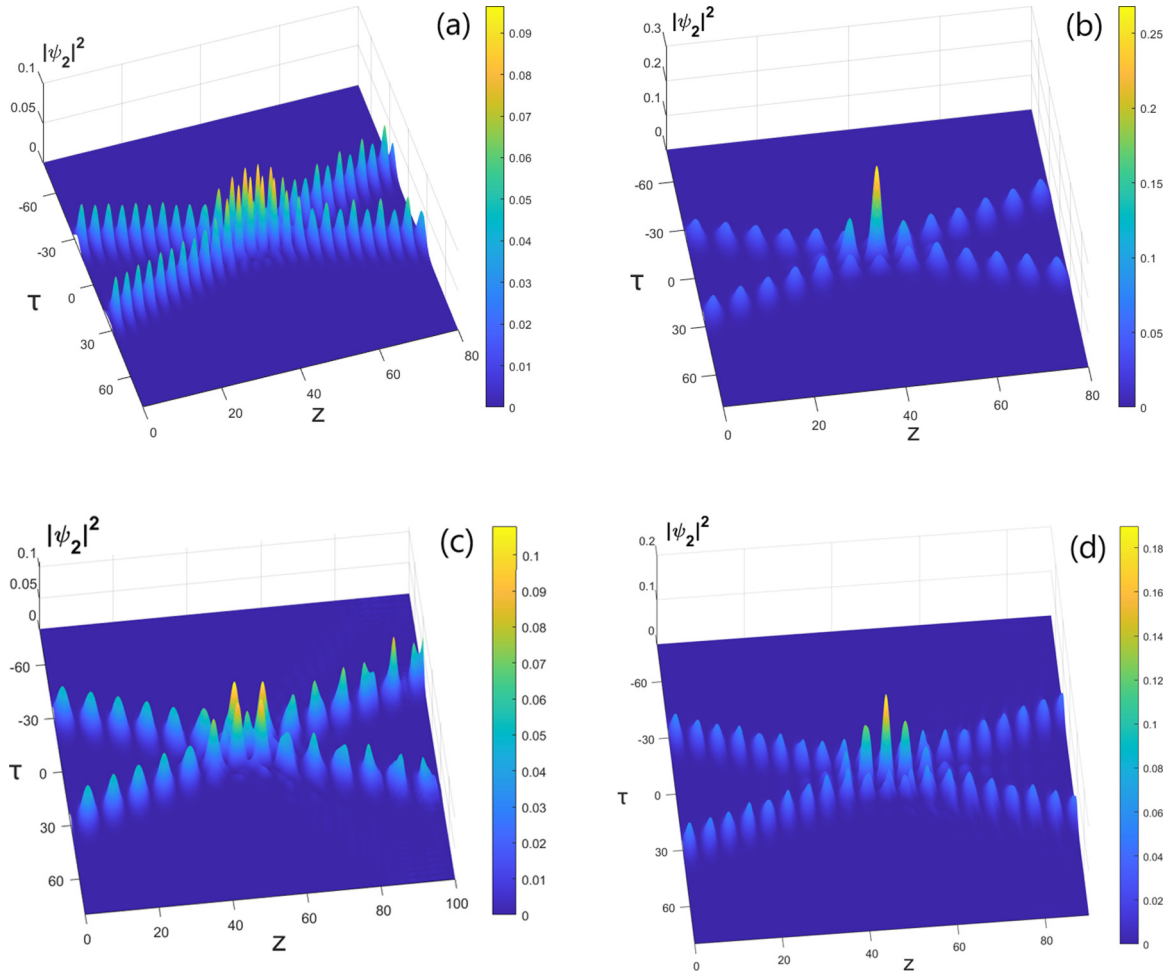


FIG. 4. Scattering of gyrating solitons in the necklace of $2N = 6$ waveguides. Shown is $|\psi_2|^2$, the power density in the second waveguide. (a, c) Collision of two “jiving” solitons with opposite sense of gyration. The initial condition is (9.2) with $\alpha = 1$, $\epsilon = 0.2$, and $V = 0.6$. Panel (a) corresponds to $\gamma = 0$ and panel (c) to $\gamma = 0.45$. In either case, the products of collision constitute solitons with the modulated flashing amplitude. (The modulation is manifested in the alternation of peaks of unequal height.) (b, d) Collision of two waltzers. The initial condition is (9.3) with $\alpha = 1$, $\epsilon = 0.2$, and $V = 0.6$. Panels (b) and (d) depict the scattering process in the system (2.1) with $\gamma = 0$ and $\gamma = 0.45$, respectively. In both cases the postcollision solitons restore their original shape.

velocities:

$$\psi_n = \frac{\epsilon}{\sqrt{3}} (v_n^{(\alpha)} + w_n^{(N-\alpha)}) \{ e^{i\frac{V}{2}\tau} \text{sech}[\epsilon(\tau + \tau_0)] + e^{-i\frac{V}{2}\tau} \text{sech}[\epsilon(\tau - \tau_0)] \}, \quad n = 1, \dots, 2N. \quad (9.1)$$

The collision of a clockwise jiving soliton and its anti-clockwise gyrating counterpart was simulated using an initial condition of the form

$$\psi_n = \frac{\epsilon}{\sqrt{3}} \{ (v_n^{(\alpha)} + w_n^{(N-\alpha)}) e^{i\frac{V}{2}\tau} \text{sech}[\epsilon(\tau + \tau_0)] + (v_n^{(N-\alpha)} + w_n^{(\alpha)}) e^{-i\frac{V}{2}\tau} \text{sech}[\epsilon(\tau - \tau_0)] \}, \quad (9.2)$$

where $n = 1, \dots, 2N$.

Despite the jiver’s weak instability, the two solitons with the same sense of gyration as well as the countergyrating soliton pair emerged from the collision unscathed. In the case of either initial condition, equation (9.1) or (9.2), the only effect of interaction was an acquired modulation of each soliton’s oscillation amplitude [Figs. 4(a) and 4(c)].

Turning to the collision of two waltzers, we set the initial condition in the form

$$\vec{\psi} = \frac{\epsilon}{\sqrt{3}} (\vec{v}^{(\alpha)} + \vec{v}^{(N)}) \{ e^{i\frac{V}{2}\tau} \text{sech}[\epsilon(\tau + \tau_0)] + e^{-i\frac{V}{2}\tau} \text{sech}[\epsilon(\tau - \tau_0)] \}. \quad (9.3)$$

In this case, the scattering was seen to be elastic. The solitons would emerge without any change in the amplitude, the velocity, or the gyrating pattern [Figs. 4(b) and 4(d)].

B. Vector Schrödinger equations

The two-component amplitude equation (4.12) and its four-component generalization (6.4) are worth commenting upon.

The vector nonlinear Schrödinger equation (4.12) has appeared in a large number of contexts and a significant wealth of knowledge about its solutions has been accumulated [27–30]. Specifically, the soliton (4.14) was proved to be stable [27,29] and localized solutions with an arbitrary number of humps were determined in addition to this fundamental

soliton [30]. By contrast, references to the four-component Schrödinger equation (6.4) seem to be lacking in the literature.

An interesting property of equations (4.12) and (6.4) is their conservativity. In particular, equation (6.4) represents a Hamiltonian system with the Hamilton function

$$H = \int [|\dot{p}_1|^2 + |\dot{p}_2|^2 + |\dot{q}_1|^2 + |\dot{q}_2|^2 + |p_1|^4 + |p_2|^4 + |q_1|^4 + |q_2|^4 - 2(|p_1|^2 + |p_2|^2 + |q_1|^2 + |q_2|^2)^2 - 4(p_1 p_2 q_1^* q_2^* + p_1^* p_2^* q_1 q_2)] dT_1,$$

where the overdot stands for $\partial/\partial T_1$. Equations (6.4) can be written as

$$i \frac{\partial p_n}{\partial Z_2} = \frac{\delta H}{\delta p_n^*}, \quad i \frac{\partial q_n}{\partial Z_2} = \frac{\delta H}{\delta q_n^*} \quad (n = 1, 2),$$

where $p_{1,2}^*$ are the momenta canonically conjugate to the coordinates $p_{1,2}$, and $q_{1,2}^*$ are the momenta conjugate to $q_{1,2}$.

Thus, despite the presence of gain and loss, the small-amplitude light pulses in the \mathcal{PT} -symmetric necklace obey Hamiltonian dynamics.

X. CONCLUDING REMARKS

A. Conclusions

When the coupled waveguides considered in this paper are linear and nondispersive—that is, when the system is modeled by the linear chain of $2N$ elements—the complex modes are given by arbitrary linear combinations of eigenvectors of the $2N \times 2N$ matrix (2.2). The addition of the nonlinearity and dispersion imposes nonlinear constraints on the coefficients of the admissible combinations. We have classified linear patterns that persist in the nonlinear dispersive necklace.

One simple pattern arising in the necklace of $2N$ linear waveguides corresponds to z -independent illumination. The pattern consists of a linear combination of $\bar{v}^{(\alpha)}$ and $\bar{v}^{(N-\alpha)}$, two eigenvectors pertaining to the repeated eigenvalue β_α (where $\alpha = 1, \dots, N-1$). A linear combination of $\bar{v}^{(\alpha)}$ and $\bar{w}^{(\alpha)}$ —the eigenvectors associated with opposite eigenvalues—describes a periodic power oscillation between odd and even waveguides. (Here α may take any value from 1 to N .) An odd-even blinking regime with the maximum waveguide power varying along the necklace is generated by a combination of four eigenvectors: $\bar{v}^{(\alpha)}$, $\bar{w}^{(\alpha)}$, $\bar{v}^{(N-\alpha)}$, and $\bar{w}^{(N-\alpha)}$ ($\alpha = 1, \dots, N-1$).

The most interesting types of structure result from combining $\bar{v}^{(\alpha)}$ with $\bar{w}^{(N-\alpha)}$, or $\bar{v}^{(\alpha)}$ with $\bar{v}^{(N)}$. With either of these choices, light propagates by switching from one guide to the next in a corkscrew fashion. A more complex, multiflash spiral is associated with a pattern comprising four eigenvectors: $\bar{v}^{(\alpha)}$, $\bar{w}^{(N-\alpha)}$, $\bar{v}^{(N)}$, and $\bar{w}^{(N)}$ ($\alpha = 1, \dots, N-1$).

Our analysis of the nonlinear dispersive structures was focused on short pulses of light. Turning on the dispersion and nonlinearity, the configuration corresponding to the z -independent illumination transforms into a constellation of $2N$ synchronized pulses. The corresponding amplitudes of supermodes are given by the soliton solutions of the one-

two-component nonlinear Schrödinger equations [Eqs. (4.6) or (4.12), respectively]. On the other hand, the nonlinear dispersive counterpart of the odd-even oscillation consists of a string of flashes. In that case, the amplitudes of the eigenvectors constituting a two-supermode pattern satisfy the system (4.12), while in a four-supermode combination, the amplitudes are solitons of the four-component equation (6.4).

The spiral patterns in the necklace of nondispersive linear waveguides persist as gyrating solitons of its nonlinear dispersive counterpart. The gyrating soliton is a light pulse that propagates along the fiber and circulates around the necklace at the same time. The soliton amplitudes of the spiral pattern combining two eigenvectors— $\bar{v}^{(\alpha)}$ with $\bar{w}^{(N-\alpha)}$, or $\bar{v}^{(\alpha)}$ with $\bar{v}^{(N)}$ —satisfy the system (4.12). The helical structure involving *four* supermodes gives rise to a multiflash gyrotor: a string of flashes with modulated brightness, revolving around the necklace as a whole. The amplitudes of the four eigenvectors $\bar{v}^{(\alpha)}$, $\bar{w}^{(N-\alpha)}$, $\bar{v}^{(N)}$, and $\bar{w}^{(N)}$ are given by the soliton solution of the four-component nonlinear Schrödinger equation (6.4).

Our numerical simulations indicate that some of the gyrating solitons are stable while some other ones are weakly unstable.

The optical necklace we considered in this paper was either conservative (no gain no loss) or \mathcal{PT} symmetric, where lossy waveguides alternate with waveguides with gain. Our perturbative construction of short-pulse solutions is equally applicable to both arrangements—as long as the gain-loss coefficient in the non-Hermitian necklace remains under the \mathcal{PT} -symmetry-breaking threshold.

The non-Hermitian necklace affords control opportunities unavailable in conservative arrays. We have shown that by varying the gain-loss coefficient one can change the length of the pulse of light, its velocity, and its sense of gyration.

B. Relation to earlier studies

It is appropriate to place our results in the context of existing literature on revolving light patterns.

The authors of Ref. [2] studied spatial solitons in the nonlinear Hermitian necklace [Eq. (2.1) without the $\partial_z^2 \psi_n$ term and with $\Gamma_n = 0$]. The localized structures of Ref. [2] are traveling solitons of the one-dimensional discrete Schrödinger equation that were transplanted from an infinite chain to a ring with a large but finite number of sites. Those structures are *not* the gyrating solitons considered in this paper. The stationary light beams of Ref. [2] are localized in n , whereas our gyrating solitons are localized in the retarded time τ .

Another class of circular patterns extensively covered in the literature comprises azimuthons in the planar nonlinear Schrödinger equation [31]. Azimuthons are ring-shaped complexes of two-dimensional solitons revolving around a common center. Unlike the gyrating solitons which are pulses traveling in waveguides, azimuthons are formed by stationary light beams in homogeneous media. Mathematically, the difference is that the azimuthon is a ring of several coexisting solitons involved in collective motion, whereas a gyrating soliton is a lone pulse revolving around the necklace on its own. The azimuthon is not constrained by any lattice, while the gyrating soliton requires a ring-shaped necklace to circulate.

Finally, we note parallels between the Hermitian spiral patterns of the present study and the rotary beams in

circular arrays reported in Ref. [10]. The principal difference between the system considered in Ref. [10] and our Eq. (2.1) with $\gamma = 0$ is that the latter is nonlinear and takes into account dispersion of pulses. These factors select particular spiral patterns that may form trajectories of the gyrating solitons.

ACKNOWLEDGMENTS

We thank Anton Desyatnikov, Boris Malomed, and Sergei Turitsyn for useful discussions. This research was supported by the National Research Foundation of South Africa (Grant No. 120844).

- [1] D. N. Christodoulides and R. I. Joseph, *Opt. Lett.* **13**, 794 (1988); J. M. Soto-Crespo and E. M. Wright, *J. Appl. Phys.* **70**, 7240 (1991); P. E. Landgridge and W. J. Firth, *Opt. Quantum Electron.* **24**, 1315 (1992); C. Schmidt-Hattenberger, U. Trutschel, R. Muschall, and F. Lederer, *Opt. Commun.* **89**, 473 (1992); K. Hizanidis, S. Droulias, I. Tsopelas, N. K. Efremidis, and D. N. Christodoulides, *Phys. Scr. T* **107**, 13 (2004); E. J. Bochove, *Opt. Lett.* **33**, 464 (2008).
- [2] W. Królikowski, U. Trutschel, M. Cronin-Golomb, and C. Schmidt-Hattenberger, *Opt. Lett.* **19**, 320 (1994).
- [3] J. Hudgings, L. Molter, and M. Dutta, *IEEE J. Quantum Electron.* **36**, 1438 (2000).
- [4] R. S. Kurti, K. Halterman, R. K. Shori, and M. J. Wardlaw, *Opt. Express* **17**, 13982 (2009).
- [5] S. Longhi, *J. Phys. B: At., Mol. Opt. Phys.* **40**, 4477 (2007).
- [6] D. J. Richardson, J. M. Fini, and L. E. Nelson, *Nat. Photonics* **7**, 354 (2013); R. G. H. van Uden, R. Amezcua Correa, E. Antonio Lopez, F. M. Huijskens, C. Xia, G. Li, A. Schülzgen, H. de Waardt, A. M. J. Koonen, and C. M. Okonkwo, *ibid.* **8**, 865 (2014).
- [7] A. B. Aceves, G. G. Luther, C. De Angelis, A. M. Rubenchik, and S. K. Turitsyn, *Phys. Rev. Lett.* **75**, 73 (1995).
- [8] B. Zhu, T. F. Taunay, M. F. Yan, J. M. Fini, M. Fishteyn, E. M. Monberg, and F. V. Dimarcello, *Opt. Express* **18**, 11117 (2010); F. Y. M. Chan, A. P. T. Lau, and H.-Y. Tam, *ibid.* **20**, 4548 (2012); S. K. Turitsyn, A. M. Rubenchik, M. P. Fedoruk, and E. Tkachenko, *Phys. Rev. A* **86**, 031804(R) (2012); P. Jason and M. Johansson, *Phys. Rev. E* **93**, 012219 (2016); C. N. Alexeyev, G. Milione, A. O. Pogrebnya, and M. A. Yavorsky, *J. Opt.* **18**, 025602 (2016); B. J. Ávila, J. N. Hernández, S. M. T. Rodríguez, and B. M. Rodríguez-Lara, *OSA Continuum* **2**, 515 (2019).
- [9] A. M. Rubenchik, I. S. Chekhovskoy, M. P. Fedoruk, O. V. Shtyrina, and S. K. Turitsyn, *Opt. Lett.* **40**, 721 (2015); I. S. Chekhovskoy, A. M. Rubenchik, O. V. Shtyrina, M. P. Fedoruk, and S. K. Turitsyn, *Phys. Rev. A* **94**, 043848 (2016); A. A. Balakin, A. G. Litvak, and S. A. Skobelev, *ibid.* **100**, 053830 (2019); I. S. Chekhovskoy, O. V. Shtyrina, S. Wabnitz, and M. P. Fedoruk, *Opt. Express* **28**, 7817 (2020).
- [10] C. N. Alexeyev, A. V. Volyar, and M. A. Yavorsky, *Phys. Rev. A* **80**, 063821 (2009).
- [11] D. Leykam and A. S. Desyatnikov, *Opt. Lett.* **36**, 4806 (2011); A. S. Desyatnikov, M. R. Dennis, and A. Ferrando, *Phys. Rev. A* **83**, 063822 (2011); D. Leykam, B. Malomed, and A. S. Desyatnikov, *J. Opt.* **15**, 044016 (2013).
- [12] Y. F. Yu, Y. H. Fu, X. M. Zhang, A. Q. Liu, T. Bourouina, T. Mei, Z. X. Shen, and D. P. Tsai, *Opt. Express* **18**, 21651 (2010); Y. Yan, J. Wang, L. Zhang, J.-Y. Yang, I. M. Fazal, N. Ahmed, B. Shamee, A. E. Willner, K. Birnbaum, and S. Dolinar, *Opt. Lett.* **36**, 4269 (2011).
- [13] C. M. Bender and S. Boettcher, *Phys. Rev. Lett.* **80**, 5243 (1998); C. M. Bender, *Contemp. Phys.* **46**, 277 (2005); *Rep. Prog. Phys.* **70**, 947 (2007); A. Mostafazadeh, *Int. J. Geom. Methods Mod. Phys.* **7**, 1191 (2010).
- [14] H. Ramezani, T. Kottos, R. El-Ganainy, and D. N. Christodoulides, *Phys. Rev. A* **82**, 043803 (2010); M.-A. Miri, A. Regensburger, U. Peschel, and D. N. Christodoulides, *ibid.* **86**, 023807 (2012); A. Regensburger, C. Bersch, M.-A. Miri, G. Onishchukov, D. N. Christodoulides, and U. Peschel, *Nature (London)* **488**, 167 (2012).
- [15] H. Ramezani, T. Kottos, V. Kovanis, and D. N. Christodoulides, *Phys. Rev. A* **85**, 013818 (2012).
- [16] A. A. Sukhorukov, Z. Y. Xu, and Yu. S. Kivshar, *Phys. Rev. A* **82**, 043818 (2010).
- [17] Z. Lin, H. Ramezani, T. Eichelkraut, T. Kottos, H. Cao, and D. N. Christodoulides, *Phys. Rev. Lett.* **106**, 213901 (2011).
- [18] I. V. Barashenkov, L. Baker, and N. V. Alexeeva, *Phys. Rev. A* **87**, 033819 (2013).
- [19] S. Longhi, *Opt. Lett.* **41**, 1897 (2016).
- [20] D. J. N. Stevens, B. J. Ávila, and B. M. Rodríguez-Lara, *Photonics Res.* **6**, A31 (2018).
- [21] D. Leykam, V. V. Konotop, and A. S. Desyatnikov, *Opt. Lett.* **38**, 371 (2013).
- [22] A. J. Martínez, M. I. Molina, S. K. Turitsyn, and Y. S. Kivshar, *Phys. Rev. A* **91**, 023822 (2015).
- [23] S. Mumtaz, R. Essiambre, and G. Agrawal, *IEEE Photonics Technol. Lett.* **24**, 1574 (2012).
- [24] A. B. Aceves, C. De Angelis, G. G. Luther, and A. M. Rubenchik, *Opt. Lett.* **19**, 1186 (1994); A. B. Aceves, C. De Angelis, A. M. Rubenchik, and S. K. Turitsyn, *ibid.* **19**, 329 (1994); E. W. Laedke, K. H. Spatschek, S. K. Turitsyn, and V. K. Mezentsev, *Phys. Rev. E* **52**, 5549 (1995).
- [25] A. V. Buryak and N. N. Akhmediev, *IEEE J. Quantum Electron.* **31**, 682 (1995).
- [26] P. L. Chu, G. D. Peng, and B. A. Malomed, *Opt. Lett.* **18**, 328 (1993); P. L. Chu, B. A. Malomed, and G. D. Peng, *J. Opt. Soc. Am. B* **10**, 1379 (1993); I. M. Uzunov, R. Muschall, M. Göllés, Y. S. Kivshar, B. A. Malomed, and F. Lederer, *Phys. Rev. E* **51**, 2527 (1995); N. F. Smyth and A. L. Worthy, *J. Opt. Soc. Am. B* **14**, 2610 (1997).
- [27] I. V. Barashenkov, S. V. Suchkov, A. A. Sukhorukov, S. V. Dmitriev, and Yu. S. Kivshar, *Phys. Rev. A* **86**, 053809 (2012).
- [28] B. A. Malomed and S. Wabnitz, *Opt. Lett.* **16**, 1388 (1991); D. J. Kaup, B. A. Malomed, and R. S. Tasgal, *Phys. Rev. E* **48**, 3049 (1993); Y. Silberberg and Y. Barad, *Opt. Lett.* **20**, 246 (1995); J. Yang and D. J. Benney, *Stud. Appl. Math.* **96**, 111 (1996); J. K. Yang, *ibid.* **98**, 61 (1997); *Phys. Rev. E* **64**, 026607 (2001); Y. Tan and J. K. Yang, *ibid.* **64**, 056616 (2001).
- [29] V. K. Mesentsev and S. K. Turitsyn, *Opt. Lett.* **17**, 1497 (1992).

- [30] M. Haelterman and A. Sheppard, *Phys. Rev. E* **49**, 3376 (1994); M. Haelterman, A. P. Sheppard, and A. W. Snyder, *Opt. Commun.* **103**, 145 (1993); J. K. Yang, *Phys. D (Amsterdam, Neth.)* **108**, 92 (1997).
- [31] A. S. Desyatnikov and Y. S. Kivshar, *Phys. Rev. Lett.* **88**, 053901 (2002); A. S. Desyatnikov, C. Denz, and Y. S. Kivshar, *J. Opt. A: Pure Appl. Opt.* **6**, S209 (2004); A. S. Desyatnikov, A. A. Sukhorukov, and Y. S. Kivshar, *Phys. Rev. Lett.* **95**, 203904 (2005); S. Lopez-Aguayo, A. S. Desyatnikov, Y. S. Kivshar, S. Skupin, W. Krolikowski, and O. Bang, *Opt. Lett.* **31**, 1100 (2006); S. Lopez-Aguayo, A. S. Desyatnikov, and Y. S. Kivshar, *Opt. Express* **14**, 7903 (2006).